CrossMark

Lupeol evokes anticancer effects in oral squamous cell carcinoma by inhibiting oncogenic EGFR pathway

Sanchita Rauth[1] · Sudipta Ray[1] · Sayantan Bhattacharyya[1] · Debapriya Ghosh Mehrotra[2] ·
Neyaz Alam[3] · Goutam Mondal[4] · Partha Nath[5] · Asoke Roy[6] · Jaydip Biswas[7] ·
Nabendu Murmu[1]

Abstract Epidermal growth factor receptor (EGFR) pathway is overexpressed in head and neck cancer (HNC). Lupeol, a natural triterpene (phytosterol found in fruits, vegetables, etc.), has been reported to be effective against multiple cancer indications. Here we investigate the antitumor effects of Lupeol and underlying mechanism in oral cancer. Lupeol-induced antitumor response was evaluated in two oral squamous cell carcinoma (OSCC) cell lines (UPCI:SCC131 and UPCI:SCC084) by viability (MTT), proliferation, and colony formation assays. Lupeol-mediated induction of apoptosis was examined by caspase 3/7 assay and flow cytometry. Effect of Lupeol on EGFR in the presence or absence of EGF was delineated by Western blot. The mRNA stability assay was performed to check the role of Lupeol on COX-2 mRNA regulation. Lupeol inhibited proliferation of OSCC cells in vitro by inducing apoptosis 48 h post treatment. Ligand-induced phosphorylation of EGFR and subsequent activation of its downstream molecules such as protein kinase B (PKB or AKT), I kappa B (IκB), and nuclear factor kappa B (NF-κB) was also found to be, in part, suppressed. Interestingly, Lupeol suppressed expression of *COX-2* at mRNA and protein level in a time-dependent manner. Primary explants from oral squamous cell carcinoma tissues further confirmed significant inhibition of proliferation (Ki67) in Lupeol-treated explants as compared to untreated control at 48 h. Together these data suggest that Lupeol may act as a potent inhibitor of the EGFR signaling in OSCC and therefore imply its role in triggering antitumor efficacy.

Keywords Oral squamous cell carcinoma · Lupeol · EGFR · COX-2

✉ Nabendu Murmu
nabendu.murmu@cnci.org.in

[1] Department of Signal Transduction and Biogenic Amines, Chittaranjan National Cancer Institute, 37 - S.P Mukherjee Road, Kolkata 700026, India

[2] Department of Molecular Pathology, Mitra Biotech, Narayana Nethralaya, Narayana Health City, Hosur Main Road, Bangalore 560099, India

[3] Department of Surgical Oncology, Chittaranjan National Cancer Institute, 37 - S.P Mukherjee Road, Kolkata 700026, India

[4] Department of Pathology, Chittaranjan National Cancer Institute, 37 - S.P Mukherjee Road, Kolkata 700026, India

[5] Department of Medical Oncology, Chittaranjan National Cancer Institute, 37 - S.P Mukherjee Road, Kolkata 700026, India

[6] Department of Pathology & Cancer Screening, Chittaranjan National Cancer Institute, 37 - S.P Mukherjee Road, Kolkata 700026, India

[7] Department of Translation Research, Chittaranjan National Cancer Institute, 37 - S.P Mukherjee Road, Kolkata 700026, India

Introduction

Oral squamous cell carcinoma (OSCC) is the sixth most common cancer in the world, accounting for 50–70 % of total cancer-related mortality [1, 2]. Many types of cancers including head and neck squamous cell carcinoma (HNSCC) show perturbation of the epidermal growth factor receptor (EGFR) which is generally associated with poor prognosis, invasion, and metastasis; thus, multiple drug targets have been developed against EGFR [3–7]. EGFR can bind to a variety of ligands such as Epidermal Growth Factor (EGF), Transforming Growth Factor-α (TGF-α), and Amphiregulin [8, 9]. EGFR stimulation leads

to autophosphorylation at a number of tyrosine residues like Tyr 1068 and Tyr 1086 in the cytoplasmic signal transduction domain, which in turn leads to AKT phosphorylation by increasing Phosphatidylinositol 3-kinase (PI3K) activity and consequently the downstream pathway of PI3K-AKT axis [10–12]. Indeed, AKT phosphorylation is also linked to activation and nuclear translocation of NF-κB [13]. Targets of NF-κB include various genes such as cyclooxygenase-2 (COX-2), matrix metalloproteinase 9 (MMP-9) and genes encoding anti-apoptotic proteins known for impacting tumor initiation, promotion, and metastasis [14–16]. The COX-2 gene is an immediate early-response gene that is shown to be induced by oncogenic growth factor signaling, carcinogens, and tumor-promoting phorbol esters [16, 17]. A large number of studies indicated that COX-2 is upregulated in transformed cells as well as in malignant tissues [18–23].

Due to frequent resistance to conventional chemotherapies or radiation therapy, the overall survival in cancers has not improved substantially over last few decades [24], thus highlighting the need to develop less hazardous and at the same time more effective new therapeutics. Unfortunately, the therapeutic effects of most of the existing anticancer drugs in clinics are limited by their general toxicity toward normal proliferating cells. In recent years, extensive studies have shown that phytochemicals can emerge as powerful remedy for various cancers and expectedly involve low cost and reduced toxicity. These agents have versatile pharmacological properties conferring antioxidative, hepatoprotective, antimutagenic, anti-inflammatory, antiarthritic, and antitumorigenic effects [25–31]. Triterpene group of phytochemicals are hydrocarbons formed by the condensation of six isoprene units and represent important structural components of plant membranes. Lupeol (Lup-20(29)-en-3h-ol) is a naturally occurring and pharmacologically active triterpene (phytosterol) found in various fruits (e.g., olive, mango, strawberry, and grapes), vegetables, and in several medicinal plants [32]. Induction of tumor differentiation and inhibition of tumor growth has been reported following Lupeol treatment in mouse melanoma and human leukemia cells [25, 33]. Studies have also shown that Lupeol inhibits the growth of hepatocellular carcinoma cells by downregulating the expression of ATP-binding cassette sub-family G member 2 (ABCG2) through interfering with the Phosphatase and tensin homolog (PTEN)-AKT signaling network [34]. In order to determine the activity of Lupeol on OSCC, we first investigated its effects on cell viability and proliferation. Furthermore, we analyzed the antitumor effects of Lupeol by targeting the activation and expression of EGFR and its downstream molecules in both in vitro cell line and patient-derived tumor explant model. We found that Lupeol has the potential to inhibit proliferation of

OSCC cell lines at least in part through suppression of EGFR signaling network that encompasses AKT, NF-κB, and COX-2. Lupeol also inhibits the proliferation of oral cancer cells of patient tumors in ex vivo. Together our findings illustrate that Lupeol has the capacity to display its potent anticancer properties in OSCC.

Methods

Reagents

Lupeol (L5632) and DMSO (D2650) were purchased from Sigma (St. Louis, MO, USA). A stock solution of Lupeol (30 mmol; MW = 426.72) was prepared by dissolving it in warm alcohol and diluting in DMSO at ratio of 1:1. For all treatment protocols, the final concentrations of DMSO and alcohol were 0.25 and 0.075 %, respectively, which is non-toxic to cells. Antibodies against phospho-EGFR (Tyr1068) (mouse monoclonal, Ab #3777) and total EGFR (mouse monoclonal, Ab #4267) were obtained from Cell Signaling Technology. Rabbit polyclonal primary antibodies against pAKT (Ser-473) (sc-7985-R), total AKT (sc-8312), pIκB (sc-8404), NF-κB p50 (sc-114), NF-κB p65 (sc-372), COX-2 (sc-7951), β-actin (sc-7210), horseradish peroxidase (HRP)-conjugated (sc-2004) and FITC-conjugated (sc-2012) goat anti-rabbit secondary antibodies were purchased from Santa Cruz Biotechnologies (Santa Cruz, CA, USA). Anti-Ki67 antibody (clone MIB-1, mouse monoclonal) was purchased from DAKO. Human recombinant EGF was obtained from Sigma (St. Louis, MO). The COX-2 and GAPDH primers were purchased from Integrated DNA Technologies. Annexin V Apoptosis Detection kit (sc-4252 AK) was obtained from Santa Cruz Biotechnology.

Cell lines and culture

Oral squamous cell carcinoma cell lines UPCI:SCC131 and UPCI:SCC084 were kindly provided by Professor Susanne M. Gollin, University of Pittsburgh, Pittsburgh, PA, USA. Both the cell lines were maintained in Minimum Essential Medium (MEM) supplemented with 10 % Fetal Bovine Serum (FBS) (Gibco, Life Technologies, USA) and incubated at 37 °C in a humidified incubator under 5 % CO_2 atmosphere. All experiments were performed after 3rd passage of cell lines. For dose-dependent studies, the 50 % confluent cells were treated with Lupeol.

MTT assay

The effect of Lupeol on the viability of cells (UPCI:SCC131 and UPCI:SCC084) was determined by

3-(4, 5-dimethylthiazol-2-yl)-2,5-diphenyltetrazolium bromide (MTT) assay. Briefly, 0.1×10^4 cells per 100 μl of media were seeded in each well of a 96-well plate and treated with different concentrations of Lupeol (5–80 μmol) for 24 and 48 h. At the end of each culture, MTT (5 mg/ml) was added to each well (10 μl/well) and plates were incubated at 37 °C for 2 h. Subsequently, the medium was replaced with 200 μl DMSO and the absorbance was measured at 570 nm using microplate reader (Tecan, infinite M200). In order to determine the IC50 value, the concentration was calculated by non-linear regression (curve fit) followed by log (inhibition) vs response equation using GraphPad Prism software.

Proliferation assay

The effect of Lupeol on proliferation of OSCC cell lines (both UPCI: SCC131 and SCC-084) was determined using p-nitro phenyl N-acetyl β-D-glucosaminidase. The cells were grown in 96-well plates and treated with increasing concentrations of Lupeol (10, 25, and 50 μmol) for 24 and 48 h, in the presence or absence of EGF (100 ng/ml). The cells were then washed with PBS and 75 μl of substrate (i.e., 53.3 mg of p-nitro phenyl N-acetyl β-D-glucosaminidase and 384 mg of citric acid dissolved in 20 ml of water and added 10 ml of 0.5 % Triton X 100, pH 5) was added to each well. The plates were incubated for 20 min at 37 °C under 5 % CO_2 atmosphere. Thereafter, 112.5 μl of developer (112 mg glycine and 55.8 mg EDTA in 30 ml of water, pH 10.4) was added to each well and the absorbance was recorded at 400 nm in microtiter plate reader.

Colony formation assay

UPCI:SCC131 and UPCI:SCC084 cells were seeded separately in 6-well plates (500 cells/well) and cultured overnight. The cells were treated with different concentrations of Lupeol (10, 25, and 50 μmol) for 24 h. The entire medium was removed from the plate and washed with sterile PBS. Fresh media was added and the cells were cultured for additional 3 days at 37 °C under 5 % CO_2 atmosphere. The resultant cell colonies were washed with PBS, fixed in 10 % formalin for 10 min, and stained with Harri's hematoxylin. Colonies, defined as >50 cells, were counted under bright field of light microscope (Leica DM1000, Germany) at 20× magnification.

Analysis of caspase 3/7 activity

UPCI:SCC131 cell line was maintained in 96-well plates and treated with increasing amount of Lupeol (10, 25, and 50 μmol) for 24 and 48 h both in the presence and absence

of EGF (100 ng/ml). The caspase assay was done as per the manufacturer's protocol (Apo-one Homogeneous Caspase-3/7 Assay, Promega). The Caspase substrate and Apo-ONE Caspase-3/7 buffer were thawed and mixed to make the Apo-ONE Caspase-3/7 reagent. For the assay, 100 μl of the reagent was added to each well of the 96-well plate containing 100 μl medium and gently mixed using a plate shaker at 500 rpm. The plate was incubated at room temperature for 30 min and fluorescence of each well was measured using a spectrofluorometer ($485_{Ex}/527_{Em}$).

Detection of apoptosis

To determine the rate of early and late apoptosis, flow cytometric analysis was done using Annexin V Apoptosis Detection kit. UPCI:SCC131 cells were seeded in six-well plates and treated with Lupeol (50 μmol). After 24, 48, and 72 h incubation, the cells were centrifuged (1500 rpm for 5 min). The pellet was resuspended in 1× assay buffer (final concentration of 1×10^6 cells/ml). Five micro liter (1 μg) Annexin V FITC and 10 μl PI were added to the mixture and incubated at room temperature in the dark for 15 min. Finally, 400 μl of 1× assay buffer was added and the samples were analyzed using BD FACSVerse™.

Western blot analysis

UPCI:SCC131 cells were seeded on six-well plates and grown overnight. Cells were pretreated with 50 μmol of Lupeol before exposure to 100 ng/ml of EGF for 30 and 60 min. Cells were lysed in ice-cold cell lysis buffer (15 mM Tris, 2 mM EDTA, 50 mM 2-mercaptoethanol, 20 % glycerol, 0.1 % Triton X-100, 1 mM PMSF, 1 mM sodium fluoride, 1 mM sodium orthovanadate, 1 μg/ml aprotinin, 1 μg/ml lenpeptin, and 1 μg/ml pepstatin). The total cell lysates (TCL) were centrifuged at 13,500 rpm at 4 °C for 15 min, and the supernatant was aliquoted in separate tubes. The protein concentration was measured using BSA kit (Thermo Scientific) as per the manufacture's protocol. Total extracts (50 μg protein/lane) were subjected to SDS-PAGE and electro-transferred to nitrocellulose membranes. The membranes were blocked with 5 % nonfat dry milk in Tris-buffered saline (20 mM Tris·HCl and 137 mM NaCl, pH 7.5) for 1 h at room temperature. The target proteins were detected by incubation of the membranes overnight with appropriate primary antibodies (Caspase 3 cleaved or active, pEGFR, pAKT1/2/3, NF-κB p50 and NF-κB p65 and COX-2). Next day, the membranes were washed using Tris-buffered saline (TBS) with 0.5 % Tween 20 and incubated with HRP-conjugated goat anti-rabbit secondary antibody. Final detection of signal was executed by using enhanced chemiluminescence kit (BioVision ECL Western Blot Substrate) according to the

manufacturer's instructions. The resulting bands were analyzed using a densitometer (Bio-Rad, GS 800). β-Actin expression was tested for confirming equal loading of proteins.

Immunofluorescence analysis

For immunofluorescence analysis, UPCI:SCC131 cells were seeded on cover slips in six-well plates and cultured overnight. Cells were treated with 50 µmol of Lupeol for 60 min, both in the presence of 100 ng/ml EGF and without EGF. The cover slips in culture of Lupeol (50 µmol) treated UPCI:SCC131 were incubated with 1:600 dilution of anti NF-κB p50 and anti p65 primary antibody after permeabilization with 0.5 % Triton X-100 and blocking with 5 % BSA. After washing with phosphate buffered saline (PBS) containing 0.5 % Tween 20, the cover slips were incubated with FITC-conjugated goat anti-rabbit secondary antibody at 1:500 dilution and incubated with DAPI. Cover slips were mounted with glycerol and imaging was performed in florescence microscope (Leica DM4000 B, Germany).

Tumor explant studies

Fresh tumor tissues were collected from a total of five primary oral squamous cell carcinoma patients (median age 52, four male and one female, site oral cavity, histologic types: moderately differentiated squamous cell carcinoma) from Chittaranjan National Cancer Institute (CNCI), Kolkata, India, immediately after surgical resection. Informed consent from patients and approval from the Research Ethics Committee of the institute were obtained. All works described here have been carried out in accordance with The Code of Ethics of the World Medical Association (Declaration of Helsinki). The tumor samples were transported to the laboratory at 4 °C, in appropriate transport buffer, for ex vivo studies and molecular and pathological evaluation. Tissues were cut into ∼2–3 mm^3 sections and cultured in 96-well plates that were coated with tumor matrix proteins and media supplemented with 2 % autologous serum [36]. Tumors were treated with Lupeol at a dose of 50 µmol, or with vehicle for 72 h. DMSO was used as a vehicle control.

Immunohistochemical analysis

Changes in Ki67 prior to and after drug treatment were evaluated by IHC using specific antibodies. Initial antigen retrieval of FFPE sections was done in antigen unmasking solution (Citrate based, Vector Laboratories) by exposure to microwave heating for 30 min. Quenching of endogenous peroxidase was done by 3 % H$_2$O$_2$ for 15 min. Protein blocking was carried out at room temperature for 1 h with 10 % goat serum. FFPE sections were incubated with primary antibody (anti-Ki67 antibody, mouse monoclonal and clone MIB-1, Dako) at room temperature for 1 h. This was followed by incubation with HRP-conjugated goat antimouse secondary antibody (Envision; Dako kit, K5007) for 1 h at room temperature. Chromogenic development of signal was done using 3,3′-diaminobenzidine (Envision; Dako kit, K5007). Tissues were counterstained with Hematoxylin (Papanicolaous solution 1a). Scoring and calculation of drug-induced inhibition in Ki67 in individual tumor explants were performed as described previously. Briefly, mean positive Ki67 cells were determined as percentage value from triplicates.

Quantitative PCR and mRNA stability assay

UPCI:SCC131 cells were treated with 50 µmol of Lupeol for 48 h. For real-time PCR, total RNA was isolated from treated cells using TRIZOL reagent according to the manufacturer's protocol and the complementary DNA (cDNA) was prepared from 2 µg of total RNA with Superscript III reverse transcriptase (Invitrogen, CA, USA). Quantitative analysis of cDNA amplification was assessed by incorporation of SYBR Green nucleic acid stain (KAPA Biosystem) into double-stranded DNA. The specific oligonucleotide primer pair for the COX-2 gene is as follows COX-2 Forward: 5′-GAATCATTCACCAGG-CAAATTG-3′ and COX-2 Reverse: 5′-TCTGTACTGCG GGTGGAACA-3′. For GAPDH, the forward primer is 5′-ATCACTGCCACCCAGAAGAC-3′ and the reverse primer is 5′-CACATTGGGGTAGGAACA C-3′. PCR was performed on a total volume of 20 µl containing 20 ng of cDNA template, 0.4 µl each of forward and reverse primers, and SYBR Green PCR Master Mix. All cDNA samples were tested in triplicate using the ABI PRISM 7500. Data were presented as relative to control cells.

For mRNA stability assay, cells were treated with 50 µmol of Lupeol for 6 h. Following treatment of the cells with actinomycin D (10 µg/ml final concentration), total RNA was extracted at specified time periods (0–180 min). The mRNA was subjected to real-time PCR as mentioned above.

Statistical analysis

All results were given as the average of three independent experiments and were presented as mean ± standard error (SEM). One-way Analysis of Variance (ANOVA) was used to determine the significance relative to the unexposed control. Differences were considered significant when $p < 0.05$.. 6

Results

Lupeol reduces cell viability and inhibits proliferation in UPCI:SCC131

In order to ascertain the anticancer effects of Lupeol on oral carcinoma in vitro, we performed a series of functional evaluation based on multiple end point assays. In this line, first we rely on the output from viability of cells following Lupeol treatment. Results from MTT assay revealed that Lupeol inhibited the viability of both the OSCC cell lines (UPCI:SCC131 and UPCI:SCC084) in a dose- and time-dependent manner with IC50 values of 26.1 and 21.42 µmol, respectively, when the cells were exposed in vitro for a duration of only 24 h (Fig. 1a–d). More than fourfold inhibition of viability was observed at this time point indicating a prompt and robust effect of the agent.

We next determined the inhibitory effect of Lupeol on proliferating cells. Treatment with Lupeol (50 µmol) significantly decreased the proliferation of both the cell lines. We observed 64 % inhibition after 24 h and 65 % inhibition after 48 h ($p < 0.01$) in UPCI:SCC-131 cells (Fig. 2a). While in case of UPCI:SCC084, about 69 % inhibition after 24 h and 75 % inhibition after 48 h was observed (Fig. 2b) and it was

found to be statistically significant ($p < 0.01$). Since it is perceived that the presence of elevated or additional growth factors or ligands in autocrine paracrine signaling loop can further trigger an aggressive proliferation cascade, we intended to understand the effect of Lupeol in regulating ligand-dependent proliferation of cells. To elucidate this, we maintained the UPCI:SCC131 cells in the presence of EGF, a ligand for cognate receptor EGFR. Interestingly, we noticed that Lupeol treatment significantly, but to a lesser extent, induced impairment of proliferation of UPCI:SCC131 cells, evincing a 52 % inhibition after 24 h and 60 % inhibition after 48 h in the presence of EGF ($p < 0.01$) (Fig. 2a). In case of UPCI:SCC084, there was 65 % inhibition after 24 h and 60 % after 48 h. Thus, it may be anticipated that Lupeol impedes proliferation both in the presence and absence of EGF in these oral squamous cell carcinoma cell lines (Fig. 2b). We further confirmed these results by colony formation assay. The results demonstrated that Lupeol inhibited colony formation of the cell lines in a dose-dependent manner, and the maximum inhibition was observed at 50 µmol concentration (Fig. 2c, d). There was an overall decrease in the number of colonies by 80 % in UPCI:SCC131 cell line and this inhibition was 85 % in UPCI:SCC084 cell line ($p < 0.01$) after to the highest dose (i.e., 50 µmol) of Lupeol (Fig. 2c, d).
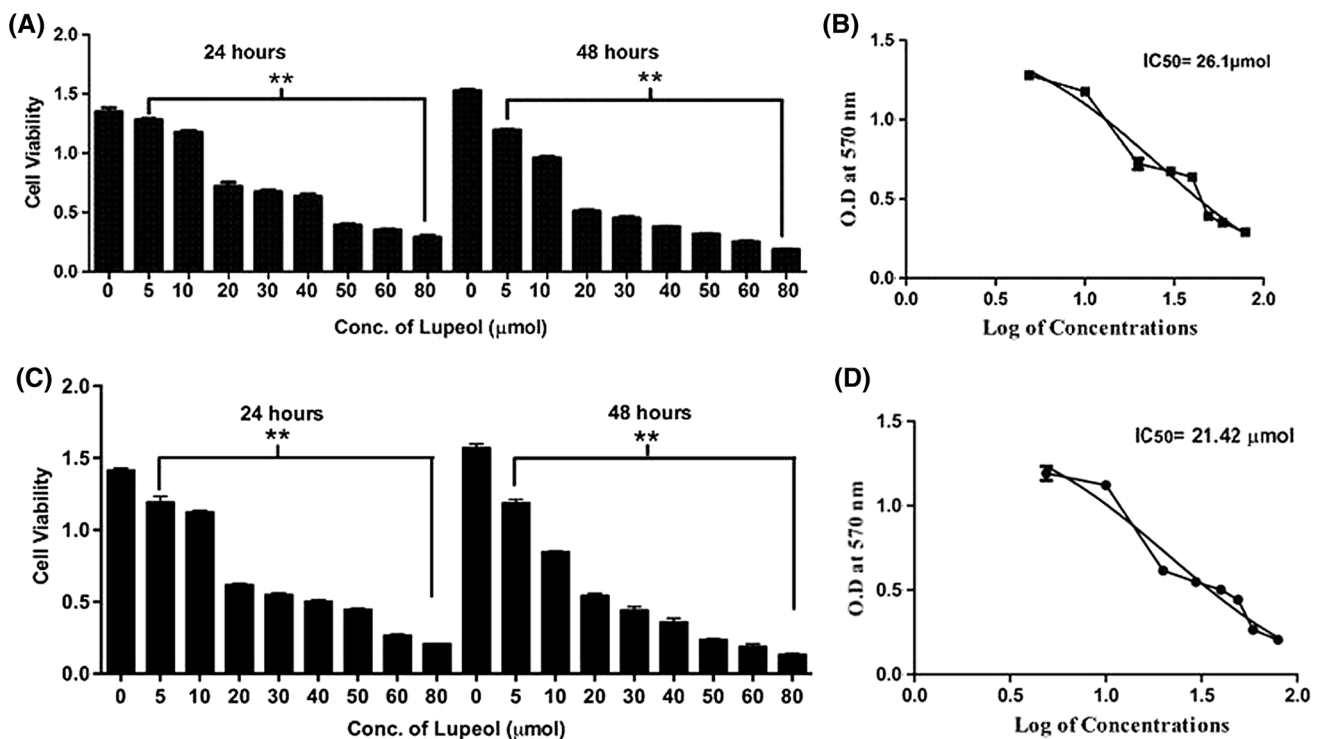

Fig. 1 Cytotoxicity of Lupeol on UPCI:SCC131 and UPCI:SCC084 cells: to evaluate drug sensitivity, UPCI:SCC131 cells were treated with different doses of Lupeol (5–80 µmol) along with control for 24 and 48 h and MTT assay was done. a Lupeol-treated cells showed a significant decrease in cell viability (**$p < 0.01$). b IC50 dose of Lupeol in UPCI:SCC131 cells was calculated to be 26.1 µmol.

Similarly, UPCI:SCC084 cells were treated with different concentrations of Lupeol (5–80 µmol) along with control for 24 and 48 h and MTT assay was done. c Viability of Lupeol-treated cells 24 and 48 h **$p < 0.01$. d IC50 dose of Lupeol in UPCI:SCC084 cells was calculated to be 21.42 µmol
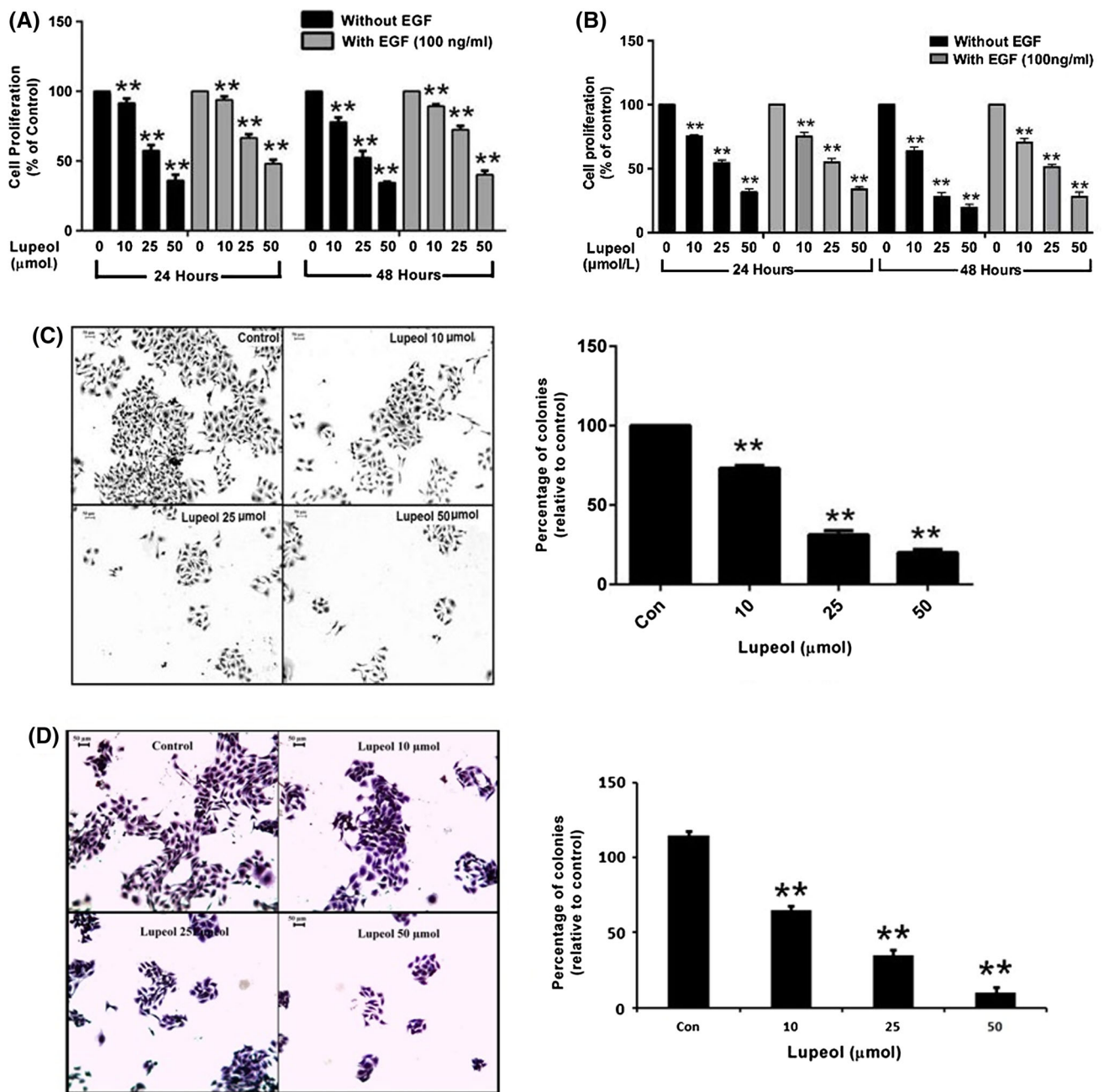
Fig. 2 Lupeol inhibited EGF-mediated proliferation and colony formation of OSCC cell lines: Cells were incubated with Lupeol (0, 10, 25, and 50 μmol) alone and with 100 ng/ml of EGF for 24 and 48 h. **a** Lupeol dose affects on the proliferation of UPCI:SCC131 cells both in the presence and absence of EGF. **b** Effect of Lupeol on proliferation of UPCI:SCC084 cell line. Data represented as mean ± SEM of three experiments with **$p < 0.01$ compared to control. **c, d** UPCI:SCC131 cells and UPCI:SCC084 were treated with different concentrations of Lupeol (0, 10, 25, and 50 μmol) for 24 h. Effect of Lupeol doses on colony formation for both UPCI:SCC131 and UPCI:SCC084 cells. Data represented as mean ± SEM of three experiments with **$p < 0.01$ compared to control

Lupeol induces apoptosis in UPCI:SCC131 cells in vitro

One of the important parameters of assessing drug efficacy in in vitro and in vivo settings is measurement of apoptosis as many drugs exert their anticancer effects by interfering with both proliferation and inducing multiple facets of

apoptosis network. From this perspective, we further looked into the effect of Lupeol on cell death. Particularly, we measured Caspase 3/7 activity after 24 and 48 h of treatment with Lupeol in the presence or absence of exogenous EGF. We found that Lupeol induced apoptosis in UPCI:SCC131 cells and exerts its effects in a dose-dependent manner both in the presence and absence of

EGF. Quantification of these results demonstrated that Lupeol treatment (50 µmol) induced a significant increase (34 %) in apoptosis after 24 h and 84 % increase after 48 h ($p < 0.01$). Moreover, Lupeol treatment (50 µmol) resulted in an increase in apoptosis (by 30 % after 24 h and 69 % after 48 h) even in the presence of EGF (Fig. 3a). These results also showed that Lupeol has the capacity to induce apoptosis in UPCI:SCC131 cells in a dose-dependent manner ($p < 0.01$).

We further ascertained this effect by performing additional evaluation metrics. Data obtained from Annexin-PI flow cytometry assay exhibited that Lupeol (50 µmol) significantly increased apoptosis in UPCI:SCC131 ($p < 0.01$) and as the time progressed maximum apoptosis (58 %) was found at 72 h after treatment (Fig. 3b, c). These data were further confirmed by Western blot using the protein lysates derived from Lupeol-treated UPCI:SCC131 cells and labeled with anti-active caspase 3 (i.e., executioner caspase) antibody. The results confirmed that with increase in time, Lupeol (50 µmol) induced apoptosis in UPCI:SCC131 cells as evidenced by increased level of active caspase 3 (Fig. 3d, e).

Lupeol inhibits EGF-mediated phosphorylation of EGFR and its downstream signaling

Data obtained from multiple end point assays prompted us to elucidate the mechanistic aspects of Lupeol-induced antitumor response in oral carcinoma cells. One of the key oncogenic signaling pathways critically involved in oral cancer is EGFR and its interaction or cross-talk at diverse levels with other molecules. We, therefore, first elucidated the role of EGFR pathway and its perturbation in effecting growth and survival of oral cancer cells in conventional in vitro model system. As shown in Fig. 4, treatment with EGF (100 ng/ml) increased the expression of phospho-EGFR and phospho-AKT after 30 and 60 min of stimulation, respectively. However, addition of Lupeol (50 µmol), in part, reversed this growth factor-mediated phosphorylation of EGFR and AKT, while levels of corresponding total proteins were found to remain unaltered.

One of the downstream effects of EGFR signaling is activation of NF-κB. Therefore, next we determined the effect of Lupeol on IκB phosphorylation (a signal of this activation cascade) and subsequent expression as well as localization of NF-κB. Western blot analysis of the protein extracts illustrated that EGF treatment for up to 60 min resulted in induction of IκB phosphorylation and NF-κB (both NF-κB1-p50 and RelA-p65 sub units) expression. In contrast, treatment with Lupeol resulted in inhibition of all these three proteins (Fig. 5a). In order to verify if Lupeol treatment hinders the NF-κB translocation to nucleus, immunofluorescence staining was performed. The resultant

data showed that supplementation with EGF increased the nuclear localization, whereas treatment with Lupeol resulted in decreased expression and blockade of translocation of both NF-κB1-p50 and RelA-p65 molecules into the nucleus in treated cells compared to control (Fig. 6).

Lupeol downregulates *COX-2* mRNA and protein expression by decreasing mRNA stability

Since induction of EGFR signaling has potential to regulate a number of other critical signaling factors and COX-2 expression is linked to the survival of oral carcinoma cells, we wanted to delineate the impact of Lupeol-induced EGFR inhibition on modulating, in parallel, COX-2 expression. RT-PCR analysis showed that Lupeol (50 µmol) decreased *COX-2* mRNA level (Fig. 7a) after 24 and 48 h of treatment. Next, we determined the effect of Lupeol on *COX-2* mRNA stability using actinomycin D. Results demonstrated that half-life of *COX-2* mRNA decreases from 64 to 30 min when compared to controls (Fig. 7b). Together these results further demonstrated that Lupeol significantly reduced the COX-2 expression (Fig. 7c) and the observed effect was enhanced with progression of the exposure time.

Lupeol inhibits tumor cell proliferation in patient-derived ex vivo system

We further elucidated the effect of Lupeol in a more relevant ex vivo explant culture model where key components of tumor microenvironment were found to be intact up to 3 days and this contextual preservation is known for impacting drug efficacy in personalized setting [35]. Patient-derived multiple tumor tissues of oral origin were cultured in slices to assess the Lupeol effects. Interestingly, Lupeol treatment showed profound decrease in proliferation of tumor cells (Ki-67) compared to control at 72 h post treatment (Fig. 8). These data showed that Lupeol can emerge as a strong anticancer molecule and their introduction as new paradigm would improve treatment outcome.

Discussion

Phytochemicals as anticancer agents hold great promise in oncology drug development and emerge as effective means in the changing anticancer therapeutic landscape. The recent reports on the effect of epigallocatechin gallate from green tea and curcumin from turmeric on growth suppression of HNSCC cell lines suggested the potential use of natural dietary substances in the treatment of HNSCC where smoking and some other habits in contrast compound the risk
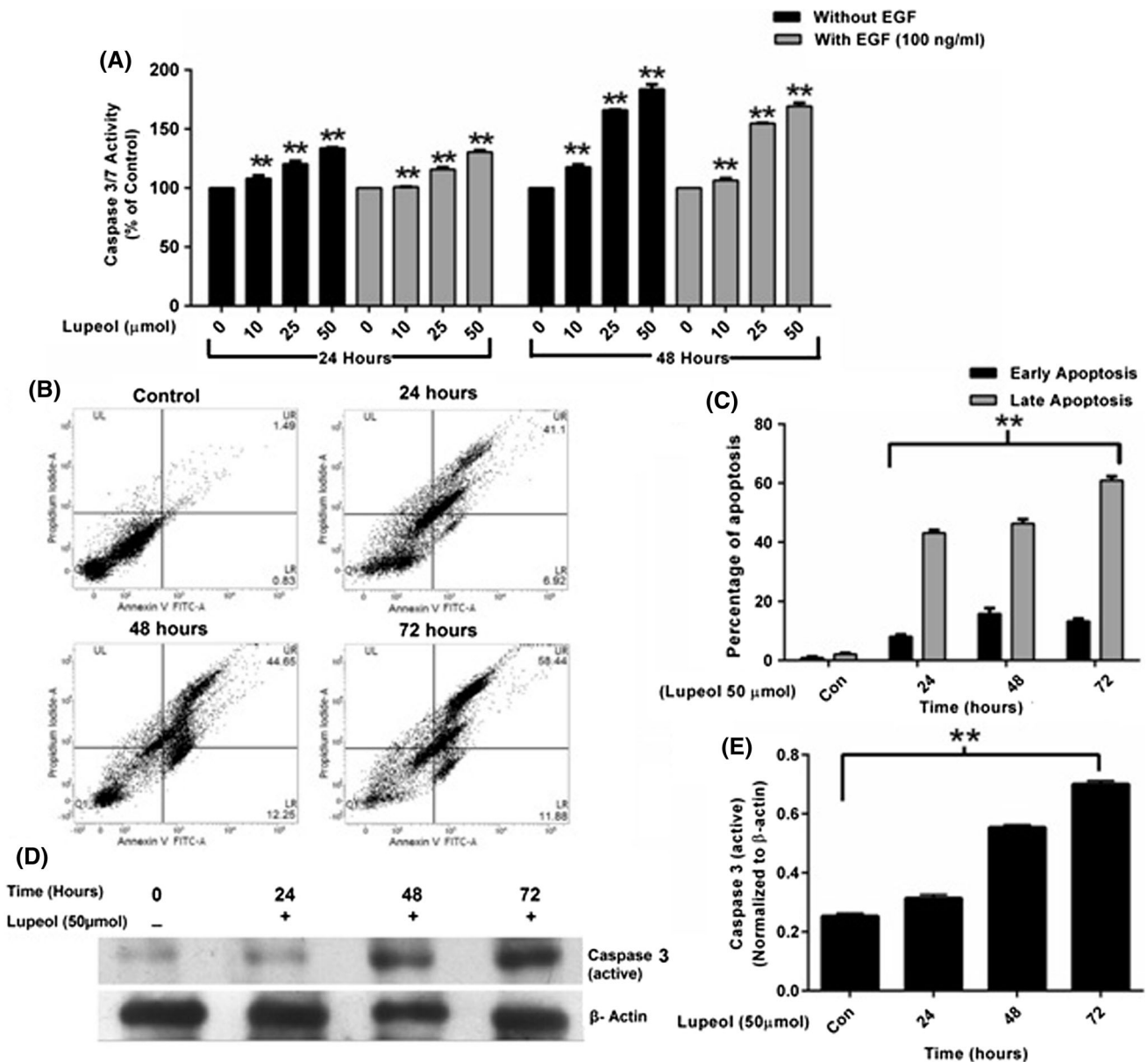
Fig. 3 Lupeol-induced apoptosis in UPCI:SCC131 cells: **a** cells were incubated with Lupeol (0, 10, 25, and 50 μmol) alone and with 100 ng/ml of EGF for 24 and 48 h. Lupeol treatment induces apoptosis in UPCI:SCC131 cells in the presence and absence of EGF. Data are expressed as percentage relative to control and mean ± SEM of three experiments (**$p < 0.01$ compared to control, $n = 3$). **b** UPCI:SCC131 cells were treated with 50 μmol of Lupeol for a specific time period (24, 48, and 72 h) and Annexin V-PI assay was performed for determine the extent of apoptosis. Lupeol induced apoptosis in UPCI:SCC131 in a time-dependent manner. **c** Graphical representation of the Annexin V/PI based on flow cytometry data. **d** UPCI:SCC131 cells were treated with 50 μmol of Lupeol for 24, 48, and 72 h. Following cell lysis, equal amounts of proteins were immunoprecipitated by caspase 3 antibody, to check the active caspase 3 expression in the treated cells. Lupeol induced caspase 3 activation with increase in time. **e** The changes in expression of caspase 3 was calculated by densitometric analysis of the proteins bands and plotted against different time periods. Data represented as mean ± SEM, $n = 3$ and **$p < 0.01$ compared to the corresponding control

of malignant development and prognosis [36]. The major advantage of these natural substances over the conventional chemotherapy is their minimal toxicity to the body and potentially broad mechanism of action. Obviously, natural agents that induce apoptosis conceivably help minimizing the chances of acquired drug resistance and decrease

frequency of mutagenesis [37]. From these perspectives, in our study, we intended to find out the activity of Lupeol on OSCC in vitro and confirm the same in a clinically relevant patient-derived ex vivo models.

We recreated two distinct experimental conditions mimicking the actively operating oncogenic pathway(s) by
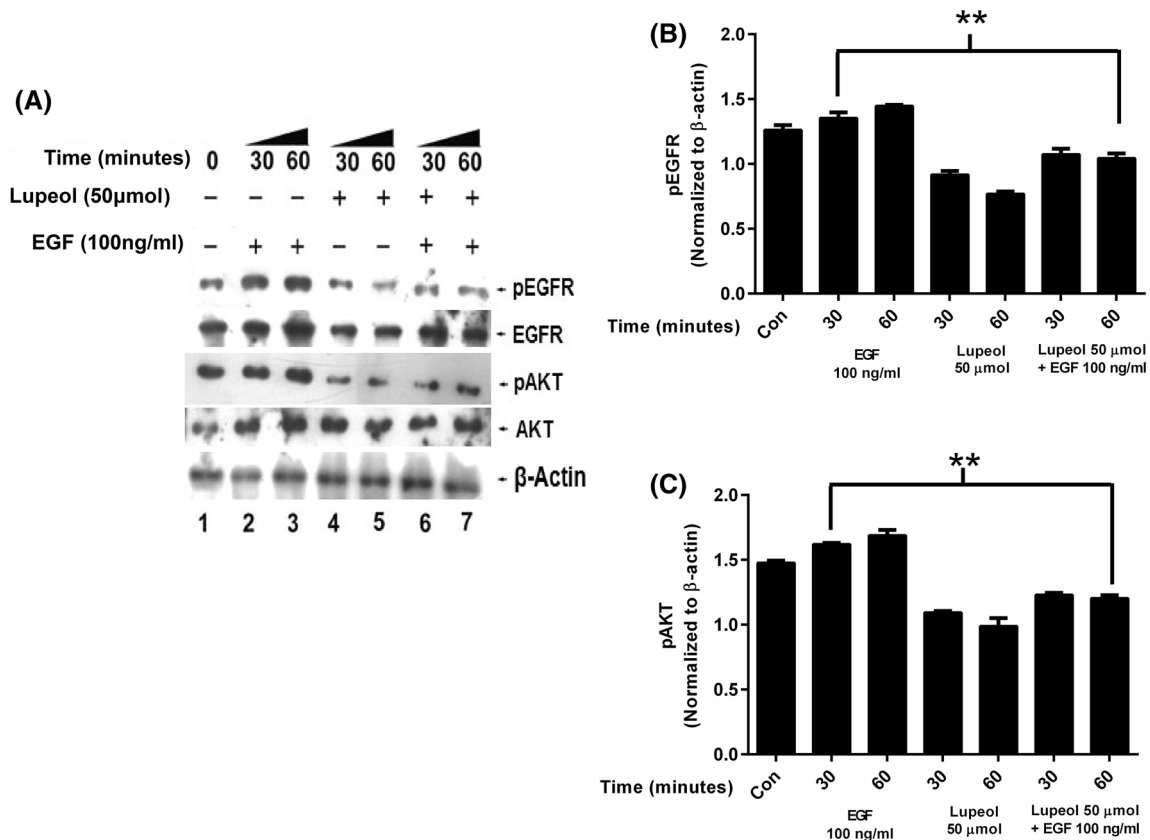
Fig. 4 Effect of Lupeol on EGFR and AKT phosphorylation on UPCI:SCC131 cells: **a** UPCI:SCC131 cells were treated with 50 μmol of Lupeol and 100 ng/ml of EGF for 30 and 60 min. Following cell lysis, equal amounts of proteins were immunoprecipitated by a specific antibody against EGFR, pEGFR (Tyr-1068), AKT and pAKT (Ser-473), total and phosphorylated status of the proteins were determined in the presence or absence of EGF. **b, c** The changes in expression of pEGFR and pAKT were calculated by densitometric analysis of the proteins bands and plotted against different time points. Data represents as mean ± SEM, $n = 3$ and **$p < 0.01$ compared to the corresponding control

using ligand-driven and ligand-deprived survival cascade to elucidate inhibitory roles of Lupeol. We found that Lupeol effectively induced antitumor response by activating diverse growth suppressing events like inhibiting cellular proliferation and inducing apoptosis in a physiologically relevant UPCI:SCC131 cell line. In many assays, these effects were found to be dose-dependent. We further checked the effect of Lupeol by repeating the viability and proliferation assays on a second OSCC line, i.e., UPCI:SCC084. It is noteworthy that the results that we obtained in case of UPCI:SCC131 (which originates from a new primary tumor) were similar to those found in UPCI:SCC084 cell line, which originates from a recurrence tumor, thus emphasizing the fact that Lupeol may be equally effective for treatment of both primary and recurrent tumors. As part of a larger oncogenic network, it is known that binding of growth factors such as EGF or TGFα to their respective receptors lead to induction of signaling networks that critically influence the proliferation, migration, survival, adhesion, and differentiation of cells [38].

Within this context, we also delineated the effects of Lupeol on proliferation of OSCC cells under both EGF-induced and corresponding basal conditions. Interestingly, our observations supported the role of Lupeol in diminishing EGFR effects under both ligand-free and ligand-enriched conditions as specifically we observed that exposure to Lupeol blocked proliferation in both the cell lines at the same concentration even when the cells were stimulated with EGF. These findings were further confirmed using a number of endpoint assays such as colony formation assay. Indeed, any anticancer molecule offers better therapeutic efficacy when it concurrently enhances multiple antigrowth and antisurvival properties of tumors. In this line, we found that Lupeol was able to trigger cellular apoptosis pathway by activating caspase 3 and 7 cascade the key effector molecules known to induce apoptosis in many cancer cells by amplifying the signals from initiator caspases, such as caspase 8 or caspase 10 [39]. Previous study has also shown that stimulation with EGF inhibits apoptosis in breast cancer cells following
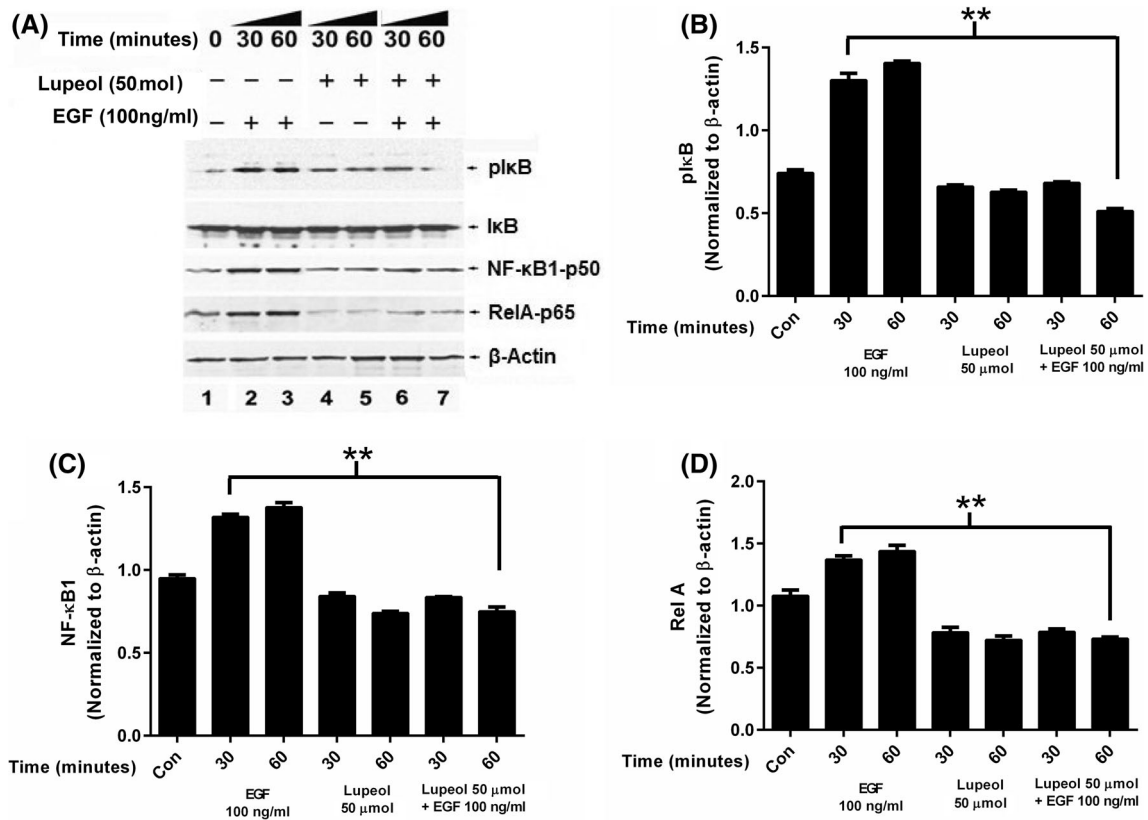
Fig. 5 Effect of Lupeol on IκB and NF-κB: **a** Western blot analysis showing treatment of cells with Lupeol along with EGF in modulating pIκB expression along with its downstream molecules NF-κB1 and Rel A at different time points. **b** The change in expression ratio of pIκB relative to control was calculated by densitometric analysis of protein bands. **c**, **d** Relative quantification of NF-κB1 and Rel A protein expression plotted against different time points. Data represented as mean ± SEM, $n = 3$ and **$p < 0.01$ compared to the corresponding control

Fig. 6 Immunofluorescence analysis of NF-κB1 and Rel A localization: EGF-mediated nuclear translocation of both the molecule NF-κB1 and Rel A was determined in the context of Lupeol treatment in UPCI:SCC131 cells by immunofluorescence microscopy. *Colors* and localization of individual proteins are depicted. (Color figure online)
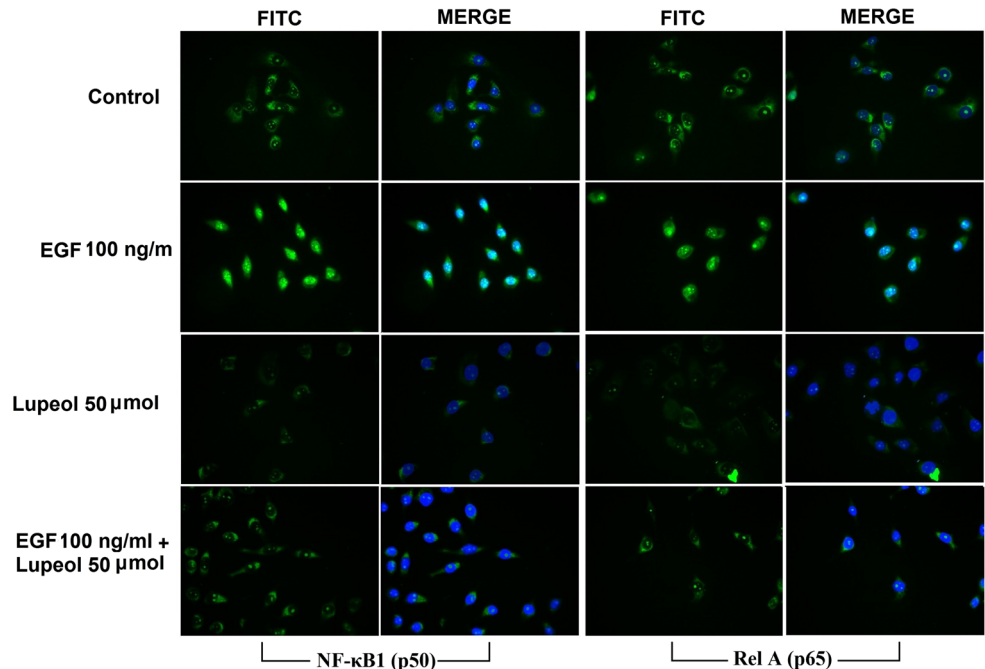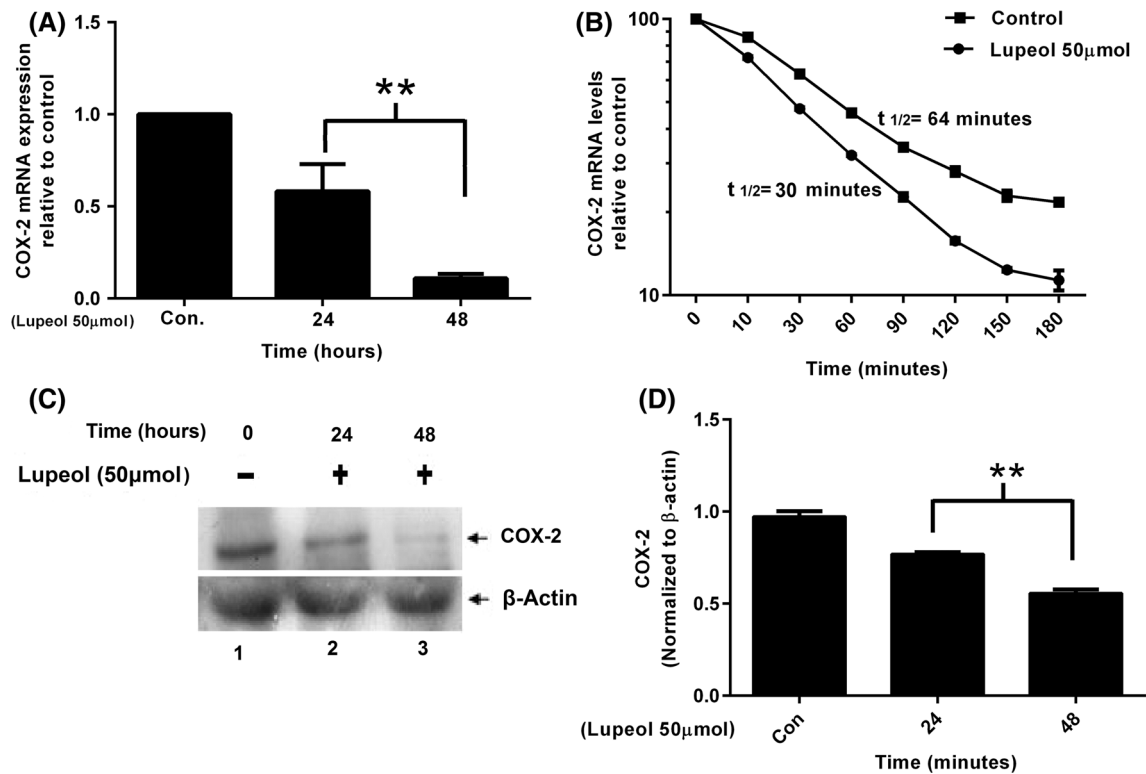
Fig. 7 Effects of Lupeol on COX-2 mRNA level, mRNA stability, and protein expression: Cultured UPCI:SCC131 cells were treated 50 μmol of Lupeol. **a** Real-time PCR analysis demonstrated the effects of Lupeol treatment on *COX-2* mRNA expression after 24 and 48 h. **b** UPCI:SCC131 cells were treated with 50 μmol of Lupeol for 0–180 min followed by treatment with actinomycin D. Lupeol treatment affects the *COX-2* mRNA half-life. **c** Western blot analysis revealed the consequence of treatment with Lupeol on COX-2 protein expression after 24 and 48 h. **d** Relative quantification of COX-2 protein bands plotted against different time periods. Data are represented as mean ± SEM, $n = 3$ and **$p < 0.01$ compared to the corresponding control
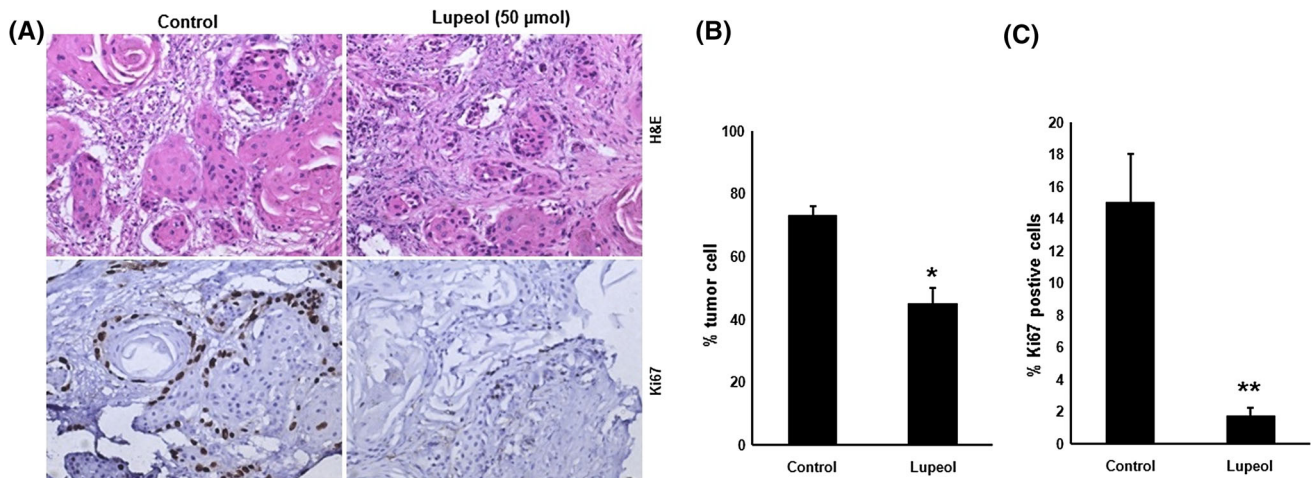

Fig. 8 Lupeol inhibits tumor cell proliferation in ex vivo settings. Primary oral squamous cell carcinoma tissue samples ($n = 5$) were sliced and cultured in explant in the presence of autologous serum- and tumor-matched matrix proteins. Tumor tissues were exposed to Lupeol (50 μmol) for 72 h. Antitumor effect was evaluated by (**a**) tumor cell content (H&E) and cell proliferation (immunohistochemistry with anti-Ki67 antibody). **b** Corresponding quantification of H&E (tumor content) and **c** Ki67 inhibition. Data are representative of total five independent experiments each performed in triplicates.*$p < 0.05$ and **$p < 0.01$ compared to the corresponding untreated controls

treatment with docetaxel [40]. We interestingly noticed that, in addition to inhibit proliferation, Lupeol induced apoptosis in UPCI:SCC131 cells, an effect that was triggered both in the presence and absence of EGF at an early time point (24 h) and maintained up to the end of treatment (48 h). These findings suggest the effectiveness of Lupeol as an anticancer therapeutic molecule.

It has been reported that EGF binding to EGFR induces a series of biochemical events including phosphorylation of EGFR in its kinase domain. Thus, the activated EGFR is known to be elevated without changing total EGFR protein level [41]. Deregulation of EGFR by overexpression or constitutive activation is associated with angiogenesis and metastasis, leading to the formulation of many therapies targeting EGFR [6]. Owing to the development of drug resistance, therapeutic monoclonal antibodies and synthetic small molecule tyrosine kinase inhibitors, directed against EGFR, often result in adverse consequences for cancer patients [42, 43]. Thus, there is the need to develop less toxic treatment approach with reduced chance of resistance attributable to broad cellular and molecular targets. This is where the natural products raised considerable interest in recent years as valuable resources to develop novel treatment options [44]. Appreciating this potential, we subsequently evaluated the activity of Lupeol on EGFR and concomitant AKT phosphorylation, both in the presence and absence of EGF, and found that Lupeol evoked inhibition of both the molecules under basal growth condition as well as in EGF-stimulated state. Activation of AKT is known to result in subsequent phosphorylation of IκB and concomitant activation of NF-κB protein [45, 46] prompting us to evaluate in parallel the effect of Lupeol on the expression of these molecules. Consistent with the upstream effects, Lupeol inhibited the phosphorylation of IκB and activation of its target molecule NF-κB both in the presence and absence of EGF as specific inhibition of translocation into nucleus was evident. Mechanistically, it was revealed that Lupeol reduced translocation of the two subunits of NF-κB (NF-κB1-p50 and RelA-p65) into the nucleus both in the presence and absence of EGF. Taken together, these results suggest that Lupeol treatment can inhibit EGFR signaling by downregulating the phosphorylation (both auto- and signal induced) of the proteins and also the subsequent activation of its downstream molecules (for e.g., AKT, IκB, and NF-κB).

Another critical aspect of Lupeol-induced antitumor response was its role to disrupt interaction of NF-κB with other pro-tumor molecules, particularly COX-2. Cyclooxygenase enzymes, also called Prostaglandin Endoperoxide Synthase, catalyze the conversion of Arachidonic acid to Prostaglandin E2 (PGE2). It has been reported that EGF-induced COX-2 and prostaglandins synthesis in oral epithelial cells occurs through EGFR pathway [47]. Upon activation, translocated NF-κB acts as a transcription factor in nucleus and induces COX-2 expression [48]. This encouraged us to further examine the activity of Lupeol on COX-2 mRNA level and protein expression. Interestingly Lupeol treatment led to the substantial decrease in *COX-2* mRNA expression along with a decrease in COX-2 mRNA half-life in UPCI:SCC131 cells which was corroborated with COX-2 protein expression. Further validation of cell line results of Lupeol in a clinically relevant ex vivo system capturing complexity of native tumor microenvironment and its diverse context fortified the scope of elucidating its potential as effective anticancer agent in clinical settings.

Conclusion

The present study provides the evidence that Lupeol treatment suppresses the tumor cell proliferation and induces their apoptosis in dose- and time-dependent manner in diverse in vitro settings. The study also provided a mechanistic insight wherein Lupeol was found to inhibit the phosphorylation of EGFR and thus activation of its subsequent critical downstream molecules such as AKT, IκB, NF-κB, and COX-2. Lupeol in a clinically relevant ex vivo explant culture model of primary OSCC demonstrated profound decrease in proliferation of tumor cells and encourages further validation in a larger cohort. Collectively, these findings are indicative of a promising anticancer function of Lupeol and may lead to new strategies that potentially ensure maximum therapeutic benefit in a clinically challenging scenario.

Compliance with ethical standards

Conflict of interest The authors declare that there is no conflict of interest.

References

1. Vokes EE, Wechselbaum RR, Lippman SM et al (2010) Head and neck cancer. N Engl J Med 328:184–194
2. Haddad RI, Shin DM (2008) Recent advances in head and neck cancer. N Engl J Med 359:1143–1154
3. Herbst RS (2004) Review of epidermal growth factor receptor biology. Int J Radiat Oncol Biol Phys 59(2 Suppl):21–26
4. Chung CH, Ely K, McGavran L et al (2006) Increased epidermal growth factor receptor gene copy number is associated with poor prognosis in head and neck squamous cell carcinomas. J Clin Oncol 24:4170–4176

5. Erman M (2007) Molecular mechanisms of signal transduction: epidermal growth factor receptor family, vascular endothelial growth factor family, kit, platelet-derived growth factor receptor, Ras. J Buon 12(Suppl 1):83–94

6. Lurje G, Lenz HJ (2009) EGFR signaling and drug discovery. Oncology 77(60):400–410

7. Seshacharyulu P, Ponnusamy MP, Jain M et al (2012) Targeting the EGFR signaling pathway in cancer therapy. Expert Opin Ther Targets 16(1):15–31

8. Yotsumoto F, Yagi H, Suzuki SO et al (2008) Validation of HB-EGF and amphiregulin as targets for human cancer therapy. Biochem Biophys Res Commun 365(3):555–561

9. Arkhipov A, Shan Y, Das R et al (2013) Architecture and membrane interactions of the EGF receptor. Cell 152(3):557–569

10. Lorimer IA, Lavictoire SJ (2001) Activation of extracellular-regulated kinases by normal and mutant EGF receptors. Biochim Biophys Acta 1538:1–9

11. Motoyama AB, Hynes NE, Lane HA (2002) The efficacy of ErbB receptor-targeted anticancer therapeutics is influenced by the availability of epidermal growth factor-related peptides. Cancer Res 62:3151–3158

12. Habib AA, Chun SJ, Neel BG et al (2003) Increased expression of epidermal growth factor receptor induces sequestration of extracellular signal-related kinases and selective attenuation of specific epidermal growth factor-mediated signal transduction pathways. Mol Cancer Res 1:219–233

13. Kane LP, Shapiro VS, Stokoe D et al (1999) Induction of NF-κB by the Akt/PKB kinase. Curr Biol 9:601–604

14. Pahl HL (1999) Activators and target genes of Rel/NF-kappaB transcription factors. Oncogene 18:6853–6866

15. Shishodia S, Potdar P, Gairola CG et al (2003) Curcumin (diferuloylmethane) down-regulates cigarette smoke-induced NF-kappaB activation through inhibition of IkappaB alpha kinase in human lung epithelial cells: correlation with suppression of COX-2, MMP-9 and cyclin D1. Carcinogenesis 24:1269–1279

16. Chandrasekar B, Bysani S, Mummidi S et al (2004) CXCLI6 signal via Gi, phosphatidylinositol 3-kinase, AKT, I kappa B kinase and nuclear factor-kappa B and induces cell–cell adhesion and aortic smooth muscle cell proliferation. J Biol Chem 279:3188–3196

17. Kelley DJ, Mestre JR, Subbaramaiah K et al (1997) Benzo[a]-pyrene up-regulates cyclooxygenase in oral epithelial cells. Carcinogenesis 18(4):795–799

18. Wilson KT, Fu S, Ramanujam KS et al (1998) Increased expression of inducible nitric oxide and cyclooxygenase-2 in Barrett's esophagus and associated adenocarcinomas. Cancer Res 58:2929–2934

19. Shim V, Gauthier ML, Sudilovsky D et al (2003) Cyclooxygenase-2 expression is related to nuclear grade in ductal carcinoma in situ and in increased in its normal adjacent epithelium. Cancer Res 63(10):2347–2350

20. Boland GP, Butt IS, Prasad R et al (2004) COX-2 expression is associated with an aggressive phenotype in ductal carcinoma in situ. Br J Cancer 90(2):423–429

21. Greenhough A, Smartt HJM, Moore AE et al (2009) The COX-2/PGE2 pathway: key roles in the hallmarks of cancer and adaptation to the tumor microenviroment. Carcinogenisis 30(3):377–386

22. Chimal-Ramirez GK, Espinoza-Sanchez NA, Utrera-Barillas D et al (2013) MMP1, MMP9, and COX-2 expressions in promonocytes are induced in breast cancer cells and correlate with collagen degradation, transformation-like morphological changes in MCF-10A acini, and tumor aggressiveness. BioMed Res Int 2013:1–15

23. Bocca C, Levolella M, Autelli R et al (2014) Expression of COX-2 in human breast cancer cells as a critical determinant of

24. Jemal AR, Siegel E, Ward T et al (2007) Cancer statistics. CA Cancer J Clin 57:43–66

25. Hata K, Hori K, Takahashi S (2002) Differentiation and apoptosis-inducing activities by pentacyclic triterpenes on a mouse melanoma cell line. J Nat Prod 65:645–648

26. Saleem M, Kaur S, Kweon MH et al (2005) Lupeol, a fruit and vegetable based triterpene, induces apoptotic death of human pancreatic adenocarcinoma cells via inhibition of Ras signaling pathway. Carcinogenesis 26:1956–1964

27. Lee TKW, Castilho A, Cheung VCH et al (2011) Lupeol targets liver tumor-initiating cells through phosphatase and tensin homolog modulation. Hepatology 53:160–169

28. Thomasset SC, Berry DP, Garcea G et al (2007) Dietary polypheolic phytochemicals- promising cancer chemopreventive agents in humans? A review of their clinical properties. Int J Cancer 120(3):451–458

29. Nguemfo EL, Dimo T, Dongmo AB et al (2009) Anti-oxidative and anti-inflammontory activities of some isolated constituents from the stem bark of Allanblackia monticola Staner L.C (Guttiferae). Inflammopharmacology 17:37–41

30. Farrand L, Oh SW, Song YS et al (2014) Phytochemicals: a multitargeted approach to gynecologic cancer therapy. BioMed Res Int 2014:1–10

31. Shukla S, Meeran SM, Katiyan SK (2014) Epigenetic regulation by selected dietary phytochemicals in cancer chemoprevention. Cancer Lett 355(1):9–17

32. Ojewole JA (2005) Antiinflammatory, analgesic and hypoglycemic effects of Mangifera indica Linn. (Anacardiaceae) stem-bark aqueous extract. Methods Find Exp Clin Pharmacol 27:547–554

33. Aratanechemuge Y, Hibasami H, Sanpin K et al (2004) Induction of apoptosis by Lupeol isolated from mokumen (Gossampinus malabarica L. Merr) in human promyelotic leukemia HL-60 cells. Oncol Rep 11:289–292

34. Lee TK, Poon RT, Wo JY (2007) Lupeol suppresses cisplantin induced nuclear factor-kappa B activation in head and neck squamous cell carcinoma and inhibits local invasion and nodal metastasis in an orthotopic nude mouse model. Cancer Res 67:8800–8809

35. Majumder B, Baraneedharan U, Thiyagarajan S et al (2015) Predicting clinical response to anticancer drugs using an ex vivo platform that captures tumour heterogeneity. Nat Commun 6:6169. doi:10.1038/ncomms7169

36. Li N, Chen X, Liao J et al (2002) Inhibition of 7,12-dimethyl-benz(a)anthrsacene (DMBA)-induced oral carcinogenesis in hamsters by tea and curcumin. Carcinogenesis 23:1307–1313

37. Ke J, Long X, Liu Y et al (2007) Role of NF-kappaB in TNF-alpha-induced COX-2 expression in synovial fibroblasts from human TMJ. J Dent Res 86(4):363–367

38. Woodburn JR (1999) The epidermal growth factor receptor and its inhibition in cancer therapy. Pharmacol Ther 82:241–250

39. Boatright KM, Salvesen GS (2003) Caspase activation. Biochem Soc Symp 70:233–242

40. Peng XH, Karna P, Cao Z et al (2006) Cross-talk between epidermal growth factor receptor and hypoxia-inducible factor-1α signal pathways increases resistance to apoptosis by up-regulating survivin gene expression. J Biol Chem 281(36):25903–25914

41. Choi SH, Mendrola JM, Lemmon MA (2007) EGF-independent activation of cell-surface EGF receptors harboring mutations found in gefitinib-sensitive lung cancer. Oncogene 26:1567–1576

42. Cappuzzo F, Bemis L, Verella-Garcia M (2006) HER2 mutation and response to trastuzumab therapy in non-small-cell lung cancer. N Engl J Med 354(24):2619–26121

epithelial to mesenchymal transition and invasiveness. Expert Opin Ther Targets 18(2):121–135

43. Nathanson DA, Gini B, Mottahedeh J et al (2014) Targeted therapy resistance mediated by dynamic regulation of extra-chromosomal mutant EGFR DNA. Sciences 343(6166):72–76

44. Kadioglu O, Jingming C, Mohamed E et al (2014) Targeting epidermal growth factor receptors and downstream signaling pathways in cancer by phytochemicals. Target Oncol 10(3):337–353

45. Cherukuri D, Goulet AC, Inoue H et al (2004) Selenomethionine regulates cyclooxygenase-2 (COX-2) expression through nuclear factor-kappa B (NF-κB) in colon cancer cells. Cancer Biol Ther 4(2):183–188

46. Mizoguchi M, Betensky RA, Batchelor TT et al (2006) Activation of STAT3, MAPK, and AKT in malignant astrocytic gliomas: correlation with EGFR status, tumor grade, and survival. J Neuropathol Exp Neurol 65(12):1181–1188

47. Mestre JR, Subbaramaiah K, Sacks PG et al (1997) Retinoids suppress epidermal growth factor-induced transcription of cyclooxygenase-2 in human oral squamous carcinoma cells. Cancer Res 57:2890–2895

48. Zamamiri-Davis F, Lu Y, Thompson JT et al (2002) Nuclear factor-kB mediates overexpression of cyclooxygenase-2 during activation of RAW 264.7 macrophages in selenium deficiency. Free Radic Biol Med 32:890–897